Simulation of a hydrogen atom in a laser field using the time-dependent variational principle

Keefer Rowan, Louis Schatzki, Timothy Zaklama, Yasumitsu Suzuki, Kazuyuki Watanabe, and Kálmán Varga

Phys. Rev. E **101**, 023313 — Published 25 February 2020

DOI: 10.1103/PhysRevE.101.023313

Simulation of a hydrogen atom in laser field using the time-dependent variational principle

Keefer Rowan

Department of Physics and Astronomy, Vanderbilt University, Nashville, Tennessee, 37235, USA

Louis Schatzki

Department of Physics and Astronomy, Vanderbilt University, Nashville, Tennessee, 37235, USA

Timothy Zaklama

Department of Physics and Astronomy, Vanderbilt University, Nashville, Tennessee, 37235, USA

Yasumitsu Suzuki

Department of Physics, Tokyo University of Science, 1-3 Kagurazaka, Shinjuku, Tokyo 162-8601, Japan

Kazuyuki Watanabe

Department of Physics, Tokyo University of Science, 1-3 Kagurazaka, Shinjuku, Tokyo 162-8601, Japan

Kálmán Varga

Department of Physics and Astronomy, Vanderbilt University, Nashville, Tennessee, 37235, USA

The time-dependent variational principle is used to optimize the linear and nonlinear parameters of Gaussian basis functions to solve the time-dependent Schrödinger equation in 1 and 3 dimensions for a one-body soft Coulomb potential in a laser field. The accuracy is tested comparing the solution to finite difference grid calculations using several examples. The approach is not limited to one particle systems and the example presented for two electrons demonstrates the potential to tackle larger systems using correlated basis functions.

I. INTRODUCTION

The experimental advances in attosecond extreme ultraviolet light pulses and intense x-ray sources [1] made possible the exploration of many time-dependent phenomena in atoms. These experiment allow, for example, the real time observation of ultrafast electron dynamics [2, 3], study of high harmonic generation [4], temporal resolution of ultrafast electron diffraction [5], attosecond imaging [6] and the monitoring of electronic coherence [7].

The need for theoretical understanding of the new experimental findings has led to intense research to develop efficient numerical solutions of the time-dependent Schrödinger equation (TDSE) [8–20]. The conventional way of solving the time-dependent Schrödinger equation is to represent the wave function in terms of basis functions or using a real space grid, and describe the dynamics with the time dependent linear coefficients. Three dimensional or radial grids [21–23] are flexible representations of time-dependent wave functions, but discrete variable representations [24–26] and B-splines [27–29] are also often used to solve the TDSE. To solve the TDSE for problems including ionization, one often needs to represent the wave function up to a few hundred Bohr distances, requiring large spatial grids or basis dimensions. The proper boundary conditions in these problems are usually enforced by using complex absorbing potentials [11, 30, 31], exterior complex scaling [32, 33], or perfectly matched layers [34].

In the conventional approaches described above the basis functions or grid is time independent and the linear coefficients are used to describe the dynamics. The goal of this paper is to explore an alternative approach using time dependent basis functions with time dependent linear coefficients. One expects that the increased flexibility allows more efficient calculations. In our approach the basis functions will be instantaneously optimized to accurately represent the rapidly changing time-dependent wave function. The optimization of the parameters of the basis function is based on the time-dependent variational principle (TDVP) [35, 36].

The time-dependent variational method was introduced by Dirac [35], extended by McLachlan [36] and

reformulated for Gaussian wave packets in Ref. [37]. The time-dependent variational method has been used in various calculations, such as in the description of the dynamical behavior of Bose-Einstein condensates [38], and in wave packet dynamics [39, 40]. Furthermore, the study of the dynamics of strongly interacting lattice bosons [41] and strongly correlated electrons [42] reflect the increasing popularity of the time dependent variational method in other fields.

The TDVP is also often used in approximating complex many-body wave functions, e.g. Fermionic Molecular Dynamics [43], Electron Nuclear Dynamics [44], and time-dependent Multi configuration Self-consistent-field calculations [45]. In these approaches, the wavefunction is approximated by Slater determinants of localized single particle orbitals. The orbitals are parameterized by dynamical variables (wave packet width, average position or momentum) and the TDVP is used to derive equation of motion for these dynamical variables.

In this work we will solve the time-dependent Schrödinger-equation by time propagation using a time-dependent basis. We will construct the basis by using Gaussian functions

$$e^{-(\alpha_r(t)+i\alpha_i(t))x^2} \tag{1}$$

allowing time dependent complex nonlinear parameters $\alpha_r(t) + i\alpha_i(t)$, and optimize the parameters by TDVP.

Gaussians basis functions are the most popular choices of quantum mechanical calculations because their matrix elements can be evaluated analytically [46, 47]. Gaussian functions however, have difficulties in reproducing the characteristic oscillatory behavior of continuum orbitals in the asymptotic region. Gaussians with complex parameters may be better suited to describe the continuum because of their inherent oscillatory nature [48]. An alternative way to extend Gaussians for problems involving ionization is to augment them with suitable functions such as B-splines [49].

The conventional way to optimize the parameters of the Gaussians is to use a gradient based Newton-Raphson approach [46, 50, 51], or use a random optimization, the so called stochastic variational method [46, 47]. Both approaches produce highly accurate ground state energies and wave functions [46]. It is not immediately clear that the TDVP is efficient and powerful enough to optimize the nonlinear parameters to reach similar accuracy. To test the TDVP for ground states, in a previous paper we used the imaginary time propagation method combined with the TDVP to solve few-particle problems [48]. It was shown, that the TDVP can be used to obtain basis functions with accuracy comparable or better than gradient based Newton-Raphson optimization. This success paves the way for the application of the TDVP to time-dependent problems, which is the objective of the present work.

To test the solution of the TDSE using time dependent Gaussian basis functions with time propagating the linear and nonlinear parameter simultaneously on equal footing, we will study the interaction of one and two electron atoms with strong laser pulses [52]. The examples include 1D and 3D Hydrogen atoms and an 1D 2 electron He atom. The Coulomb interaction will be represented with a Gaussian or soft Coulomb potential to avoid the singularity in 1D and to allow the direct comparison with the results of finite difference grid calculations.

II. FORMALISM

A. Time-dependent variational principle

A variational ansatz (a linear combination of basis functions depending on some parameters) for a time dependent wave function in a general form can be written as:

$$\psi(\mathbf{x}, \mathbf{q}, t), \tag{2}$$

where $\mathbf{q}(t) = (q_1(t), q_2(t), \ldots, q_K(t))$ is a set of linear and nonlinear variational parameters, $\mathbf{x}$ is a set of spatial coordinates describing the system (e.g. the position of the electrons), and K is the total number of unknown variables, the sum of number of linear and nonlinear basis parameters. To simplify the notation we drop the spatial dependence and use the following shorthand notation:

$$\psi(t) = \psi(\mathbf{q}, t). \tag{3}$$

The time-dependent Schrödinger equation,

$$i\frac{d}{dt}\psi(t) = H\psi(t) \tag{4}$$

will be solved by the McLachlan variational method [36]. In this approach, the norm of the deviation between the right-hand and the left-hand side of the time-dependent Schrödinger equation is minimized with respect to the trial function. The quantity

$$I = ||i\dot{\phi}(t) - H\psi(t)||^2 \to \min \tag{5}$$

is to be varied with respect to ϕ only, and then the equivalency $\dot{\psi} \equiv \phi$ is enforced. At time t the wave function is known and its time derivative is determined by minimizing I. In case of $I = 0$, an exact solution exists, but the approximation in the expansion of $\psi(t)$ leads to $I > 0$ values.

The variations of I with respect to ϕ gives the equations of motion:

$$\left\langle \frac{\partial\psi}{\partial\mathbf{q}} \middle| i\dot{\psi} - H\psi \right\rangle = 0\ . \tag{6}$$

This equation can be used to determine the (linear and nonlinear) variational parameters.

B. Parameter optimization

The equation of motion, Eq. (6) is a set of equations

$$\left\langle \frac{\partial\psi}{\partial q_j}\middle| i\dot{\psi} - H\psi \right\rangle = 0 \qquad j = 1, 2, \ldots, K \quad , \tag{7}$$

which, using

$$\dot{\psi} = \sum_{k=1}^{K} \frac{\partial\psi}{\partial q_k}\dot{q}_k \tag{8}$$

can be rewritten as

$$i\sum_{k=1}^{K}\left\langle \frac{\partial\psi}{\partial q_j}\middle|\frac{\partial\psi}{\partial q_k}\right\rangle \dot{q}_k - \left\langle \frac{\partial\psi}{\partial q_j}\middle| H\psi\right\rangle = 0 \qquad j = 1, 2, \ldots, K. \tag{9}$$

By defining

$$M_{ij} = \left\langle \frac{\partial\psi}{\partial q_i}\middle|\frac{\partial\psi}{\partial q_j}\right\rangle \ , \tag{10}$$

and

$$v_i = \left\langle \frac{\partial\psi}{\partial q_i}\middle| H\psi\right\rangle \ . \tag{11}$$

we can write the equation of motion in matrix form as:

$$iM\dot{\mathbf{q}} = \mathbf{v}. \tag{12}$$

This can be solved to express the time dependence of the variational parameters as

$$\dot{\mathbf{q}} = -iM^{-1}\mathbf{v}. \tag{13}$$

There are various established ways to solve such first order linear differential equations [53–55], and approximations allowing larger time steps such as a Runge-Kutta approach can be used, but we elected to use the Euler method for time propagation for simplicity. The Euler method is a simple first order approximation of the time derivative and leads to

$$\mathbf{q}(t + \Delta t) = \mathbf{q}(t) - iM^{-1}\mathbf{v}\Delta t, \tag{14}$$

where Δt is the time step.

C. Hamiltonian and basis functions

We will test the approach by using a Hamiltonian describing a particle in a laser field in length gauge

$$H = -\frac{1}{2}\left(\frac{d^2}{dx^2} + \frac{d^2}{dy^2} + \frac{d^2}{dz^2}\right) + V(x, y, z) + F(t)z, \tag{15}$$

where $F(t)$ is the time dependent electric field pulse, which is defined as:

$$F(t) = E_0 e^{-(t-T)^2/\tau^2}\cos(\omega t). \tag{16}$$

We define two different types of basis functions to represent the time-dependent wave function. The first one takes on the form:

$$g_i = c_i z^{n_i} g_{\alpha_i}(x) g_{\alpha_i}(y) g_{\beta_i}(z) = c_i z^{n_i} e^{-\alpha_i(x^2+y^2)-\beta_i z^2}, \tag{17}$$

where

$$g_\sigma(x) = e^{-\sigma x^2} \tag{18}$$

is a one dimensional Gaussian and will be referred to as polynomial times Gaussian (PTG). The second basis is a plane wave times Gaussian (PWG):

$$g_i = c_i g_{\alpha_i}(x) g_{\alpha_i}(y) g_{\beta_i}(z) e^{kz} = c_i e^{-\alpha_i(x^2+y^2)-\beta_i z^2+kz}. \tag{19}$$

The parameters of the Gaussians are kept equal in the x and y direction due to the cylindrical symmetry of the potential. In one dimensional (1D) test calculations $\alpha = 0$ is used to reduce the basis to 1D.

The variational parameters form a vector,

$$\mathbf{q}(t) = \begin{pmatrix} c(t) \\ \alpha(t) \\ \beta(t) \end{pmatrix} = \begin{pmatrix} c_1(t) \\ \vdots \\ c_N(t) \\ \alpha_1(t) \\ \vdots \\ \alpha_N(t) \\ \beta_1(t) \\ \vdots \\ \beta_N(t) \end{pmatrix}, \tag{20}$$

in the case of PTG and a similar vector can be defined for PWG. For PTG, the values of n_k must be set to be integers. The variational trial function is

$$\psi(t) = \psi(\mathbf{q}(t)) = \sum_{k=1}^{N} c_k(t)\phi_k(t) = \sum_{k=1}^{N} g_k(t). \tag{21}$$

To illustrate the flexibility of the Gaussian basis in time-dependent calculations, we solve the TDVP equation (Eq. (12)) analytically for a free particle in Appendix A. This case can be used to test the time step and matrix elements in the numerical calculations.

As the example in Appendix A and Eq. (14) show, the parameters of the basis functions become complex during the time propagation. This shows that to use the TDVP for time propagation one has to allow complex basis functions, which in our case is a Gaussian function with complex parameters.

A Gaussian with a complex parameter can be written as:

$$e^{-(\alpha_r + i\alpha_i)x^2} = e^{-\alpha_r x^2}\left(\cos\left(\alpha_i x^2\right) + i\sin\left(\alpha_i x^2\right)\right). \tag{22}$$

This function is an oscillatory function with a Gaussian envelope, and seems to greatly enhance the flexibility of

the basis function [48]. To make the integrals of the matrix element convergent, α_r should be positive, which is not explicitly guaranteed in the time propagation of Eq. (14), but in our numerical examples it was always satisfied. The reason for preservation of the positive sign is not clear. In the simple example of the free wave packet, Eq. (A10) shows that if one starts with a real positive $\alpha(0)$ (which is a natural choice to describe a localized initial state), then the real part of $\alpha(t)$ will remain positive. We could not derive an analytical proof for a more general case.

We will use two potentials to test the approach. A single Gaussian potential,

$$V = -V_0 e^{-\mu(x^2+y^2+z^2)}, \tag{23}$$

with $V_0 = 1$ and $\mu = 0.1$ a.u., and a soft Coulomb potential,

$$V = -\frac{1}{\sqrt{x^2+y^2+z^2+a^2}}, \tag{24}$$

the value of a used in the calculations is listed in Table I. We will use the soft Coulomb potential because the Coulomb potential cannot be easily used in grid calculations [56] and its use is problematic in 1D [57]. In the case of the PWG basis, the soft Coulomb potential is expanded into 50 Gaussians to facilitate the analytical calculations of the matrix elements. Soft Coulomb potential has been often used in model calculations of ionization of atoms [58, 59].

In 1D test cases, the condition $x = y = 0$ is set in the potential and $\alpha = 0$ is used in the basis function with 1D kinetic energy. The matrix elements of these basis functions can be calculated analytically as it is shown in Appendices B, C and D.

D. Time propagation of the wave function

In Eq. (20) we have defined $\mathbf{q}(t)$ for Gaussian basis functions by separating the linear parameters $(c_1(t), c_2(t), \ldots, c_N(t))$ of the wave function from the nonlinear ones (that appear in the exponents) $(\alpha_1(t), \ldots, \alpha_N(t), \beta_1(t), \ldots, \beta_N(t))$. Equation (14) defines the time propagation of both linear and nonlinear parameters of the wave function. With the exception of very small time steps, the simple first order finite difference approximation is not expected to be accurate enough to preserve the norm of the wave function. To alleviate this problem, we only use Eq. (14) to time propagate the nonlinear parameters and we update the linear parameters separately to preserve the norm. One can view this as an optimization of the basis functions by updating the nonlinear parameters using TDVP. We then time propagate the wave function on the updated basis.

We have a set of basis function in time t, $\phi_k(t)$, which is time-propagated to time $t + \Delta t$ to become $\phi_k(t + \Delta t)$ using Eq. (14). Both of these sets of basis functions can be used to represent the wave function at time t:

$$\psi(t) = \sum_{k=1}^{N} \hat{c}_k(t,t)\phi_k(t) = \sum_{k=1}^{N} \hat{c}_k(t,t+\Delta t)\phi_k(t+\Delta t). \tag{25}$$

In this equation $\hat{c}_k(t,t)$ is known as we know the wave function at time t (and it is not calculated using Eq. (14)). The unknown $\hat{c}_k(t,t+\Delta t)$ coefficients can be easily derived by defining the overlap of the basis functions

$$S_{ij}(t,t') = \langle \phi_i(t) | \phi_j(t') \rangle \tag{26}$$

and multiplying Eq. (25) with $\psi_i(t)$. The result is:

$$\hat{c}_i(t,t+\Delta t) = \sum_{j=1}^{N} S^{-1}_{ij}(t,t) \sum_{k=1}^{N} S_{j,k}(t,t+\Delta t)\hat{c}_k(t,t). \tag{27}$$

Now we know the linear combination coefficient of the wave function $\psi(t)$ at time t on the optimal basis $\phi_k(t+\Delta)$, so we can time propagate the wave function in the conventional way using

$$\psi(t+\Delta t) = e^{-iH\Delta t}\psi(t) \tag{28}$$

to calculate $\hat{c}_k(t+\Delta t, t+\Delta t)$. We choose the numerically stable Crank-Nicolson approach to update the coefficients:

$$\hat{C}(t+\Delta t, t+\Delta t) = \frac{S(t+\Delta t,t+\Delta t) - \frac{i}{2}H(t+\Delta t,t+\Delta t)}{S(t+\Delta t,t+\Delta t) + \frac{i}{2}H(t+\Delta t,t+\Delta t)}\hat{C}(t,t+\Delta t), \tag{29}$$

where $\hat{C}^T = (\hat{c}_1, \ldots, \hat{c}_N)$ and

$$H_{ij}(t,t') = \langle \psi_i(t) | H | \psi_j(t') \rangle. \tag{30}$$

This approach significantly improves the stability of the approach and allows larger time steps.

III. CALCULATIONS

A. Ground state

Before the time propagation we need to calculate the ground state (without the laser field). In the time propagation that will be the initial state at $t = 0$. To calculate the ground state the parameters of the Gaussians will be defined with a geometric progression,

$$\frac{1}{\sqrt{\alpha_i}} = a\nu^{i-1}, \tag{31}$$

with $a = 0.5$ and $\nu = 1.3$. For the ground state calculation, we will use $n = 0$ for the PTG basis and $k = 0$ in the PWG basis. For 1D grid calculation, $N = 5000$ equidistant grid points are used with $h = 0.125$ grid spacing ,

Basis	N	Potential	Energy
1D PTG	30	Gauss	-0.79526702
1D PWG	20	Gauss	-0.79526702
1D Grid	5000	Gauss	-0.79526702
1D PWG	20	Soft Coulomb ($a = 1$)	-0.66977138
1D Grid	5000	Soft Coulomb ($a = 1$)	-0.66977138
1D PWG	30	Soft Coulomb ($a = 2$)	-0.50000000
1D Grid	5000	Soft Coulomb ($a = 2$)	-0.50000000
3D PWG	30	Soft Coulomb ($a = 1$)	-0.27489135
3D Grid	4465200	Soft Coulomb ($a = 1$)	-0.27461231

TABLE I. Ground state energies (in a.u.). The basis dimension is N for the PWG and PTG, and the number of grid points in the 1D and 3D grid case.

and a $N = 61 \times 61 \times 1200$ size grid with $h = 0.25$ is used in 3D. While very fine grid spacing can be used in 1D, it must be larger in 3D due to the increase in computational cost. These grid parameters define a 600 a.u. box size in 1D and 300 a.u. size in 3D in the direction of the laser field. The atom is placed in the middle of the box. These simulation boxes are sufficiently large to propagate the wave function during the laser field without reflection from the boundaries. The grid dimensions are listed in Table I. We note that due to the cylindrical symmetry of the system one could use cylindrical coordinates instead of Cartesian 3D ones. This would significantly reduce the computational cost for the 3D H atom. In this work our main goal is to demonstrate the accuracy of the time-dependent Gaussian basis and for that purpose the 3D grid approach can be simply implemented and provides sufficient precision.

The ground state energies are listed in Table I. These energies were calculated by diagonalization of the PTG and PWG case. In the case of the grid calculations, the ground state energy was calculated by the conjugate gradient method using the codes of [60]. There is an excellent agreement in 1D, and a slight difference between the PWG and the grid calculation in 3D. While agreement can be achieved with a finer grid, there are more computational constraints the finer the grid becomes. We only used the PTG for the Gauss potential, so the PTG ground state energy for other cases is not shown.

B. Time propagation

Two different laser pulses are used in the calculation. The first (see Fig. 1), laser A, has only a few cycles and moves the electron to one direction as will be shown later. The second, laser B, has many cycles and moves the electron almost symmetrically left and right. The time step is $\Delta t = 0.001$ a.u. in 1D calculations, and $\Delta t = 0.0005$ a.u. in the 3D calculations for both the PWG and the grid. The PTG requires a smaller time step as we will discuss later.

The PTG ground state calculation was restricted to $n = 0$ and to make a starting PTG basis for time propagation, the basis will be doubled by adding $n = 1$ states with the same β_i parameters as of the $n = 0$ states. These states are needed because the laser field operator $F(t)z$ matrix elements are only nonzero for basis states for even $n_i + n_{i'} + 1$. To start the calculation from the ground state, the linear coefficients of the $n_i = 1$ basis states will be set to zero. States with $n > 1$ do not seem to improve the calculation. The PWG basis does not need any modification and one can start the computation from the ground state wave function.

The electron density, $|\psi(x,t)|^2$, after time propagation up to t=100 a.u. are compared in Fig. 2 in the case of the Gaussian potential. The agreement between the grid and the PWG calculations are excellent. In the asymptotic region where the density becomes smaller than 10^{-4}, the two approaches do not fully agree. This is partly because of numerical noise, which can be decreased with a smaller time step, and partly due to the grid spacing.

Test calculations show that PTG basis can only be used with smaller time steps ($\Delta t = 0.00001$ a.u.) to produce the same results as the grid and PWG. This is because this basis easily becomes nearly linearly dependent (large overlap between basis functions), especially in the 1D case, which makes the calculation of the inverse of M difficult. The other difficulty is choosing the optimal number of basis states with $n = 0$ and $n = 1$. It is still useful to consider the PTG basis as an alternative test, especially that in 3D the Coulomb potential can be analytically calculated for this basis (see Appendix C).

Figures 3, and 4 show the energy and the occupation probability of the ground state as a function of time. The occupation probability is defined as:

$$P(t) = |\langle\psi(0)|\psi(t)\rangle|^2. \tag{32}$$

The energy and the occupational probability are in excellent agreement for the grid, PTG, and PWG basis functions for both laser fields. The ionization probability is equal to 1 minus the occupation probability of the bound states. In these examples the excited state occupation probabilities are much smaller than the occupation probability of the ground state, so the ionization probability is $\approx 1 - P(t)$ (the bound state excitations are negligible). Laser A strongly ionizes the system and the ground state occupation becomes about 0.3 after the pulse. This means (see Fig. 2) that the tail of the wave function has large amplitude far away form the center of the potential, but the complex Gaussian basis is flexible enough to represent this.

The next example is a test for a soft Coulomb potential. Since the PTG requires much smaller time step, we exclude it from the discussion from now. Figures 5 and 6 show that the approach works well for the soft Coulomb potential as well. Comparing Figs. 3 and 4 to 5 and 6 show that the effect of the laser field is very similar in both the Gauss and soft Coulomb potentials. The electron is slightly less bound in the soft Coulomb potential

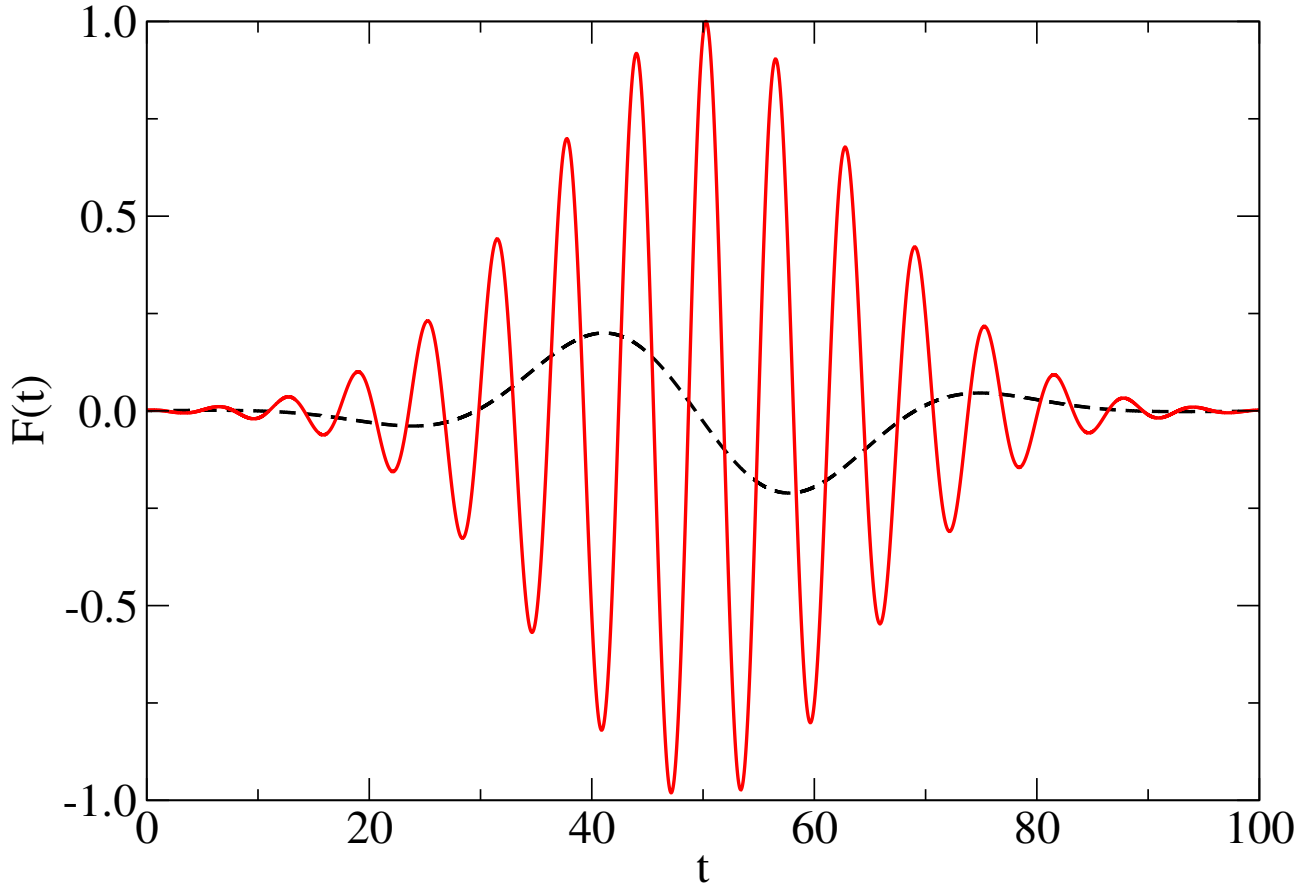

FIG. 1. The laser fields used in the calculation, laser A, $E_0 = 0.25, \tau = 20.5, \omega = 1.0/2\pi, T = 50$ (black dotted line); laser B, $E_0 = 1.0, \tau = 20.5, \omega = 1.0, T = 50$ (red line)

and the laser causes larger excitation and ionization.

The last 1D example is the calculation of the photoelectron spectra (PES). To calculate the PES we will use the approach proposed in Ref. [61]. This approach calculates the wave function $\psi(R,t)$ in time at a fixed sampling point R far away from the nucleus. This function is time Fourier transformed to energy space

$$\psi(R,E) = \int_0^\infty \mathrm{e}^{iEt}\psi(R,t)dt. \tag{33}$$

Using this function we can define

$$P_R(E) = |\psi(R,E)|^2 \tag{34}$$

which represents the probability of having an electron at R with energy E. This approach has been tested by comparing to other definitions of PES in Ref. [62]. We have calculate the PES of the 1D H atom using the benchmark test of Ref. [62]. This model uses a soft Coulomb potential with $a = 2$ and a 25 fs long laser field. The laser parameters are listed in Fig. 3 of [62]. We have used a large simulation box for the grid calculations (5000 grid points with grid spacing of 0.4 a.u.) to avoid reflections from the boundary. One could add a complex absorbing potential to avoid reflections (as it has been done in Ref. [62]), but that could slightly change the PES. Moreover, as we do not use complex absorbing potential in the TDVP PWG approach, it is better to compare the calculations without absorbing boundary. We have used $N = 30$ Gaussians (see Table I.), which is a larger basis than the ones used in the previous examples, because the laser pulse in the PES calculation is longer. The PES was calculated at $R = 500$ a.u. from the center.

The results presented in Fig. 7 are in very good agreement with Ref. [62], the grid and the Gaussian basis produces very similar PES. This is not surprising considering that as we have shown before, the wave functions calculated on the grid and using TDVP with Gaussians is nearly identical (see Fig. 2.)

The next example covers the case of soft Coulomb in 3D for lasers A and B, which are illustrated in Figs. 8 and 9. The agreement between the grid and PWG calculations is still very good, although the necessary time step to reach accuracy is smaller for PWG than in 1D. The grid calculation would converge with a time step that is 10 times larger, but we used the same time step for both grid and PWG for consistency. However, even with a larger time step, the grid calculation is computationally demanding due to its large grid size.

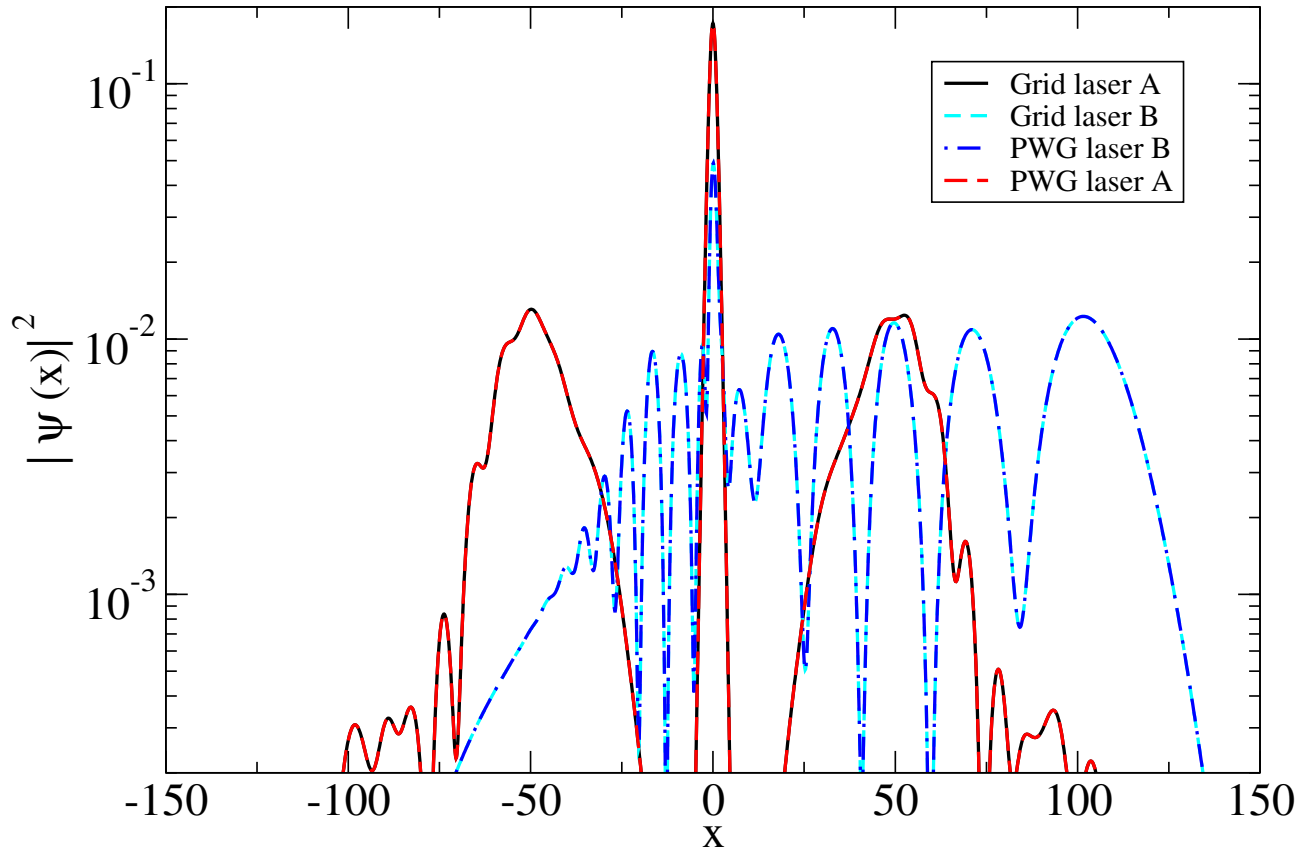

FIG. 2. Electron densities in Gaussian potential at $t = 100$ a.u. for laser A and laser B.

We have also tested a restricted PTG basis, constraining the Gaussian to be spherically symmetric by choosing $\alpha = \beta$ in Eq. (19). Test calculations for shorter, weaker pulses show good agreement between this restricted basis and the grid calculations, but this basis is not flexible enough for accurate calculations in the test examples presented in this work. Despite this, the result is still noteworthy because it may lead to an extension of Gaussian atomic orbitals for weak fields.

To test the applicability of the approach for larger systems we have considered a two electron system in 1D with the Hamiltonian

$$H = -\frac{1}{2}\frac{d^2}{dx_1^2} - \frac{1}{2}\frac{d^2}{dx_2^2} \tag{35}$$

$$- 2V(x_1) - 2V(x_2) + V(x_1 - x_2) + F(t)(x_1 + x_2), \tag{36}$$

with a Gaussian potential, $V(x) = e^{\mu x^2}$, $\mu = 0.1$ a.u.. The basis function is taken in the form

$$g_i = c_i e^{-\alpha_{1i}x_1^2 - \alpha_{2i}x_2^2 + \beta_i x_1 x_2 + k_{1i}x_1 + k_{2i}x_2} \tag{37}$$

with six variational parameters, $\alpha_{1i}, \alpha_{2i}, \beta_i, k_{1i}, k_{2i}$ and c_i, $(i = 1, \ldots, N$. The two particles are assumed to be distinguishable (one electron with spin up and one with spin down).

The energy of the two electron system as the function of time is shown in Fig. 10. The convergence was checked by using different starting basis sets and different basis dimensions. $N = 15$ basis functions with $\Delta t = 0.0001$ a.u. yields well converged results. Figure 11 show the snapshots of the two-electron density. At $t = 0$ the electrons are confined to the potential well around the origin. The laser field moves them out of the well towards the positive direction ($t = 30$ a.u. in Fig. 11), and then back toward the origin. After the peak of the laser field (in Fig. 11, $t = 50$ a.u.) there are two peaks that appear in the density. This corresponds to a configuration where the first electron's probability distribution has a maximum close to the origin, while the second electron's probability distribution has two maxima, which are left and right with respect to the origin.

IV. SUMMARY

We have used the TDVP to solve the time-dependent Schrödinger equation using time-dependent Gaussian basis functions. The TDVP optimizes the linear and the nonlinear parameters on the same footing. The results are compared to those of grid calculations and the accuracy to the present approach is demonstrated. We have tested various forms of basis functions including Gaussians multiplied by polynomials, plane waves, and

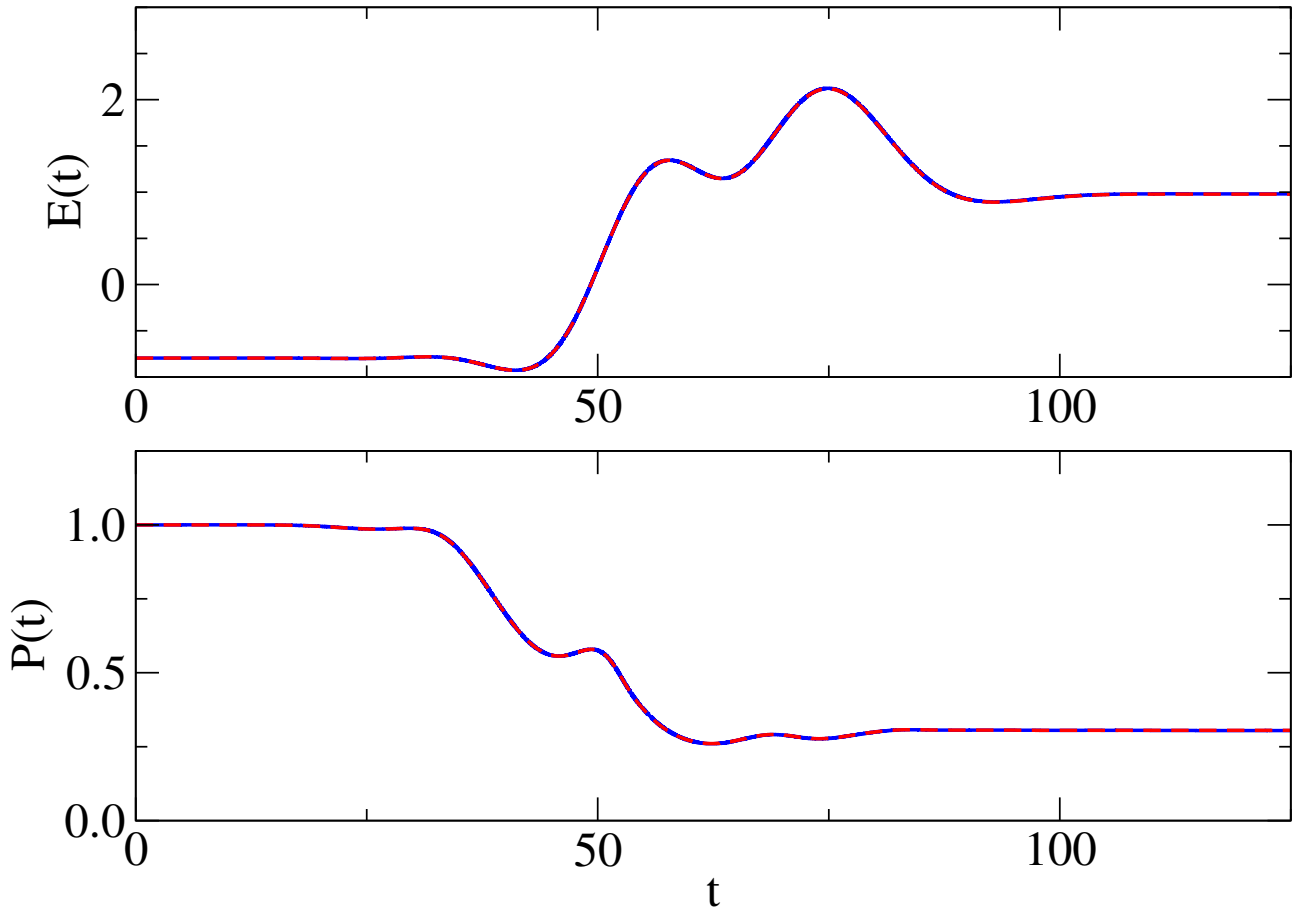

FIG. 3. Gaussian potential with laser field A in 1D. Top: Energy as a function of time for grid (solid blue line), PWG (red dashed line) and PTG (black dotted line). Bottom: Ground state occupation probability as a function of time for grid (solid blue line), PWG (red dashed line) and PTG (black dotted line). The three lines are indistinguishable in the resolution of the figure.

non-spherical Gaussians. The complex parameters of the Gaussians make the basis functions flexible enough to represent oscillatory wave functions. In addition, several potentials and laser fields were used to test the approach for different degree of ionization.

The approach has several advantages. First, a simple Gaussian basis can be used to solve time-dependent problems, which may be useful in various electronic structure codes. Second, the number of basis functions needed is considerably smaller than the number of grid points required to represent a wave function. The tradeoff is similar to the solution of a time independent problem comparing atomic orbital like basis functions to a real space grid. The atomic functions can be used to form a smaller basis, but the resulted Hamiltonian matrix is dense and the basis is nonorthogonal. The dimension of the real space grid is high, but it is an orthogonal representation with very sparse Hamiltonian. The Gaussian basis facilitates analytical expressions for the matrix elements, while the grid approach approximates the derivatives with finite differences. A further advantage is that no boundary conditions need to be enforced, and the TDVP automatically generates the Gaussians to represent the wave function in space. As the free Gaussian wave packet example (Appendix A) shows, the wave function can propagate from any given point to any desired distance without artificial reflections. In principle, a complex absorbing potential can also be used, in which case the number of Gaussian basis states may be less, because the wave function only need to be represented in a well defined region. The approach can be extended to larger systems using Explicitly Correlated Gaussians [46]. The TDVP example using explicitly correlated Gaussians for a time-dependent 2 electron system presented in this paper shows promising results.

The main disadvantage is that the basis needs to be carefully initialized, otherwise large overlap between basis functions can make the inversion of the M matrix in Eq. (10) difficult. This can possibly be alleviated by using a singular value decomposition for calculation of the inverse. It is also somewhat difficult to determine a sufficient number of basis functions and their desired initial parameters to minimize error during time propagation.

The approach can be improved in several ways. Chief

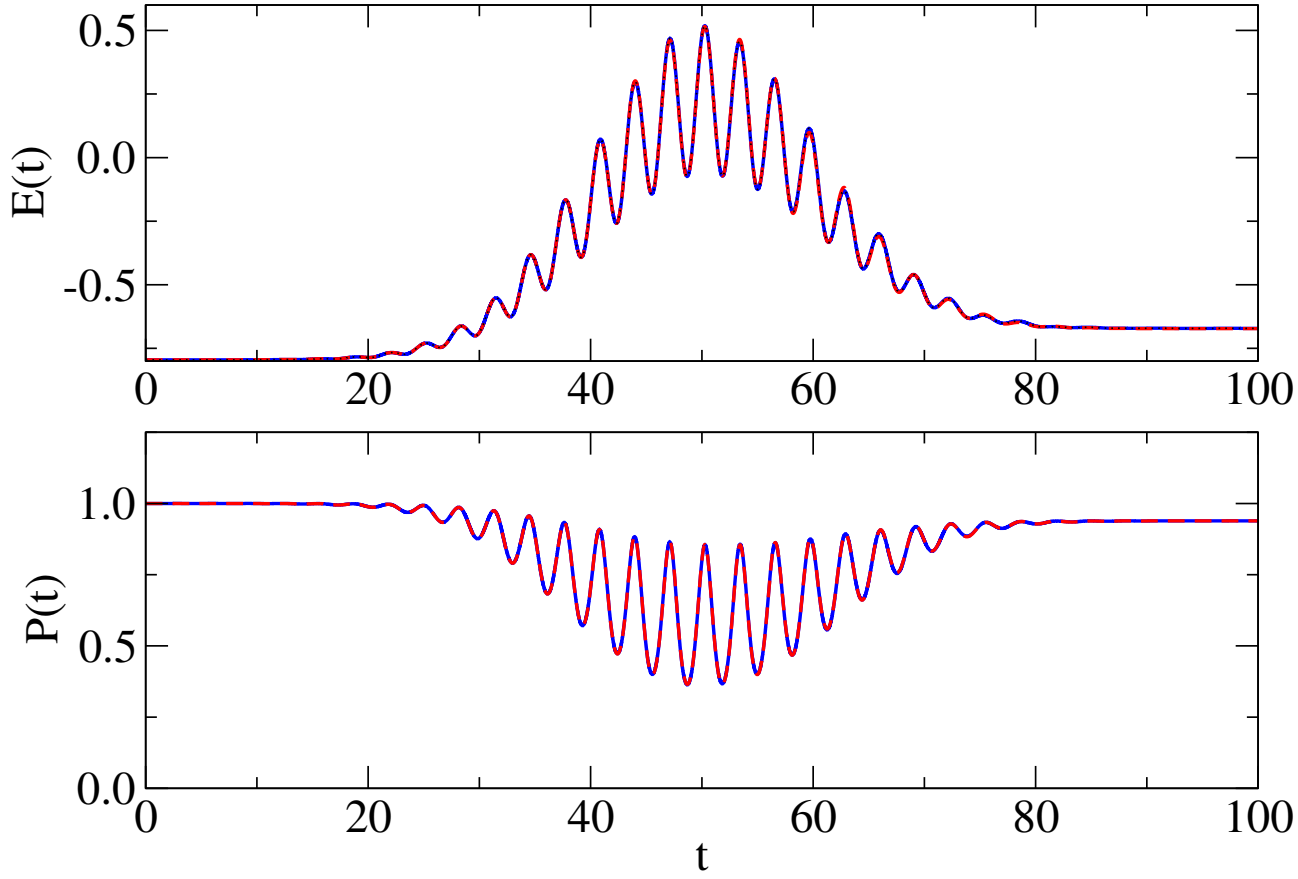

FIG. 4. Gaussian potential with laser field B in 1D. Top: Energy as a function of time for grid (solid blue line), PWG (red dashed line) and PTG (black dotted line). Bottom: Ground state occupation probability as a function of time for grid (solid blue line), PWG (red dashed line) and PTG (black dotted line). The three lines are indistinguishable in the resolution of the figure.

among them, the simple first order time propagation should be replaced with a more accurate approach. The approach can also benefit from adaptive time steps, using larger time step for smooth regions of the time dependent potential and smaller time steps where the potential has abrupt changes. Both of these improvements would allow for larger time steps and faster calculation. One can also design some scheme to prune the number of Gaussians and add new Gaussians as needed. Finally, another possibility is to refit the wave function with a completely new set of Gaussians after a certain time interval to exclude ill-behaved basis states.

V. ACKNOWLEDGMENT

This work has been supported by the National Science Foundation (NSF) under Grant No. IRES 1826917.

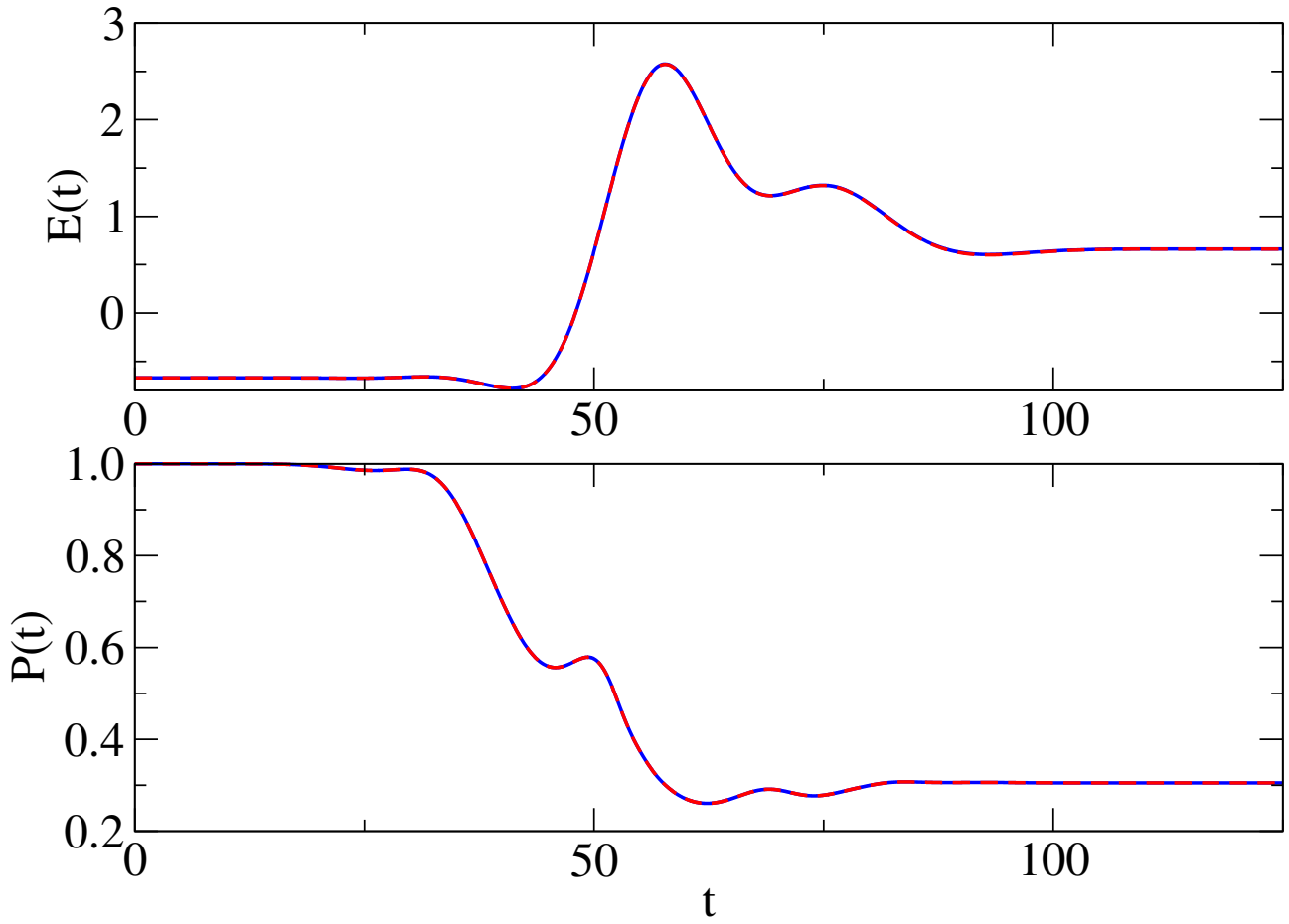

FIG. 5. Soft Coulomb potential with laser field A in 1D. Top: Energy as a function of time for grid (solid blue line), PWG (red dashed line). Bottom: Ground state occupation probability as a function of time for grid (solid blue line), PWG (red dashed line).

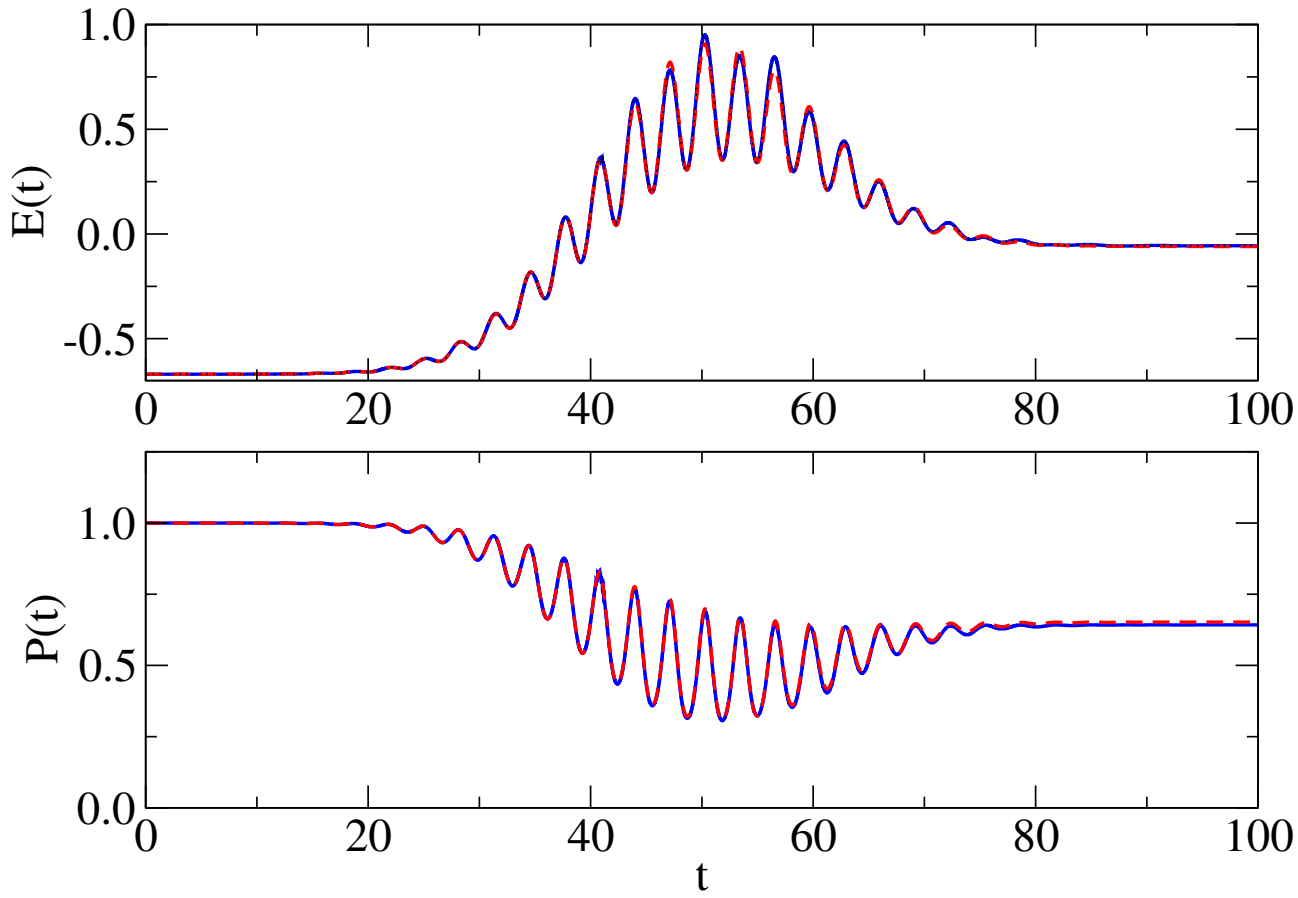

FIG. 6. Soft Coulomb potential with laser field B in 1D. Top: Energy as a function of time for grid (solid blue line), PWG (red dashed line). Bottom: Ground state occupation probability as a function of time for grid (solid blue line), PWG (red dashed line).

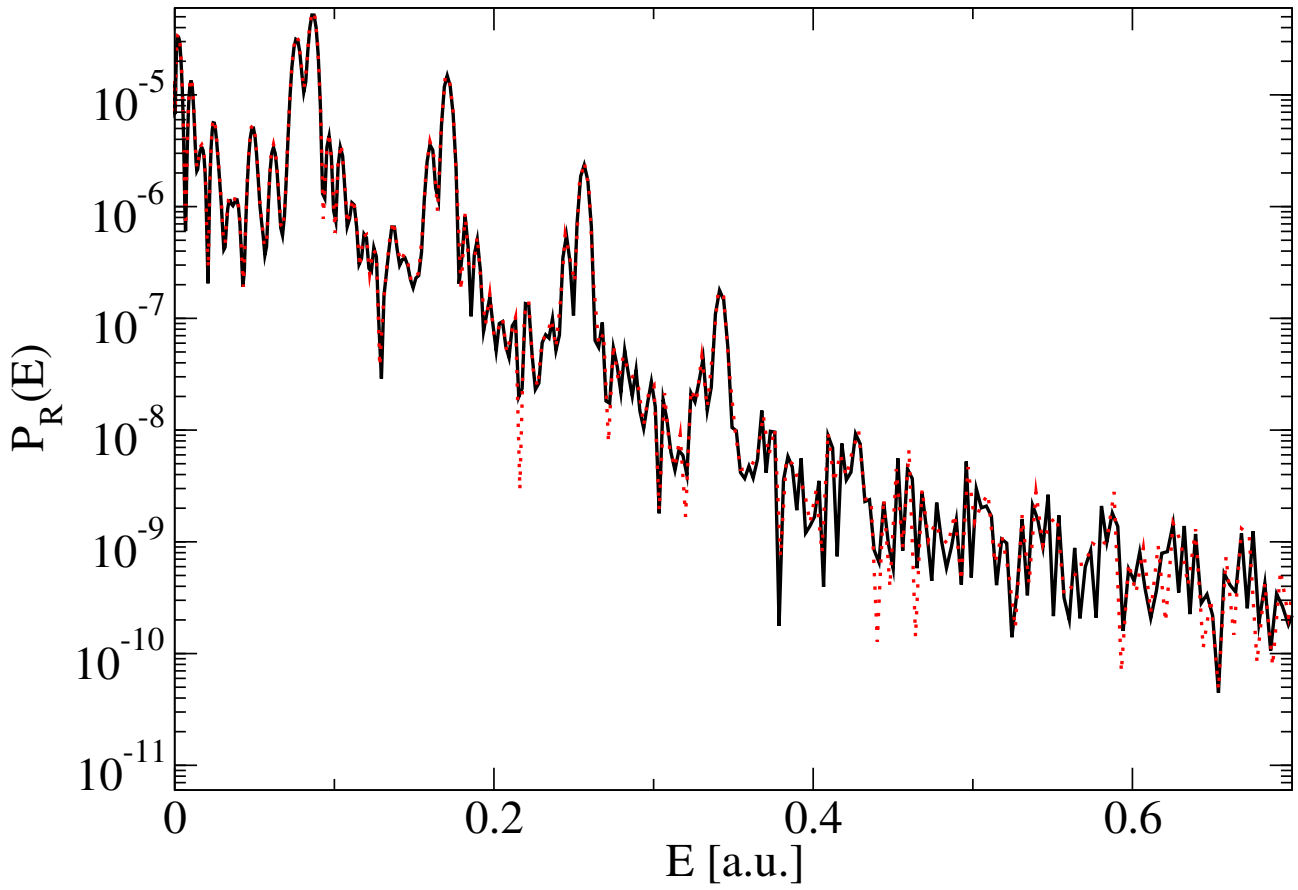

FIG. 7. PES calculated by PWG (solid black line) and grid (red dotted line). The 1D model presented in Ref. [62] was used in the calculation. The grid calculation uses the same parameters as the sampling point method in Ref. [62], and show the same characteristic spectrum, peaks appearing at integer multiples of $\omega = 0.0856$.

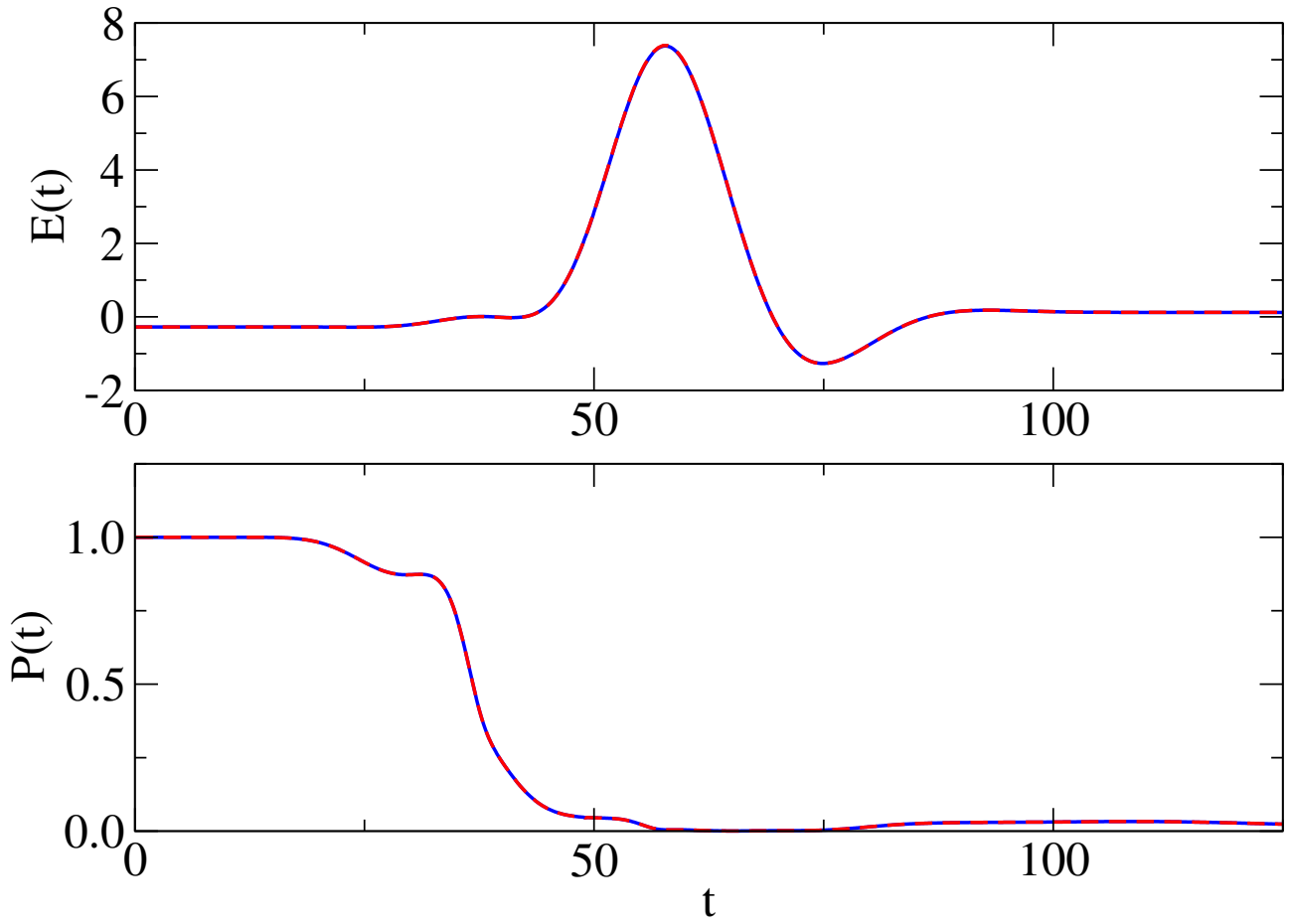

FIG. 8. Soft Coulomb potential with laser field A in 3D. Top: Energy as a function of time for grid (solid blue line), PWG (red dashed line). Bottom: Ground state occupation probability as a function of time for grid (solid blue line), PWG (red dashed line).

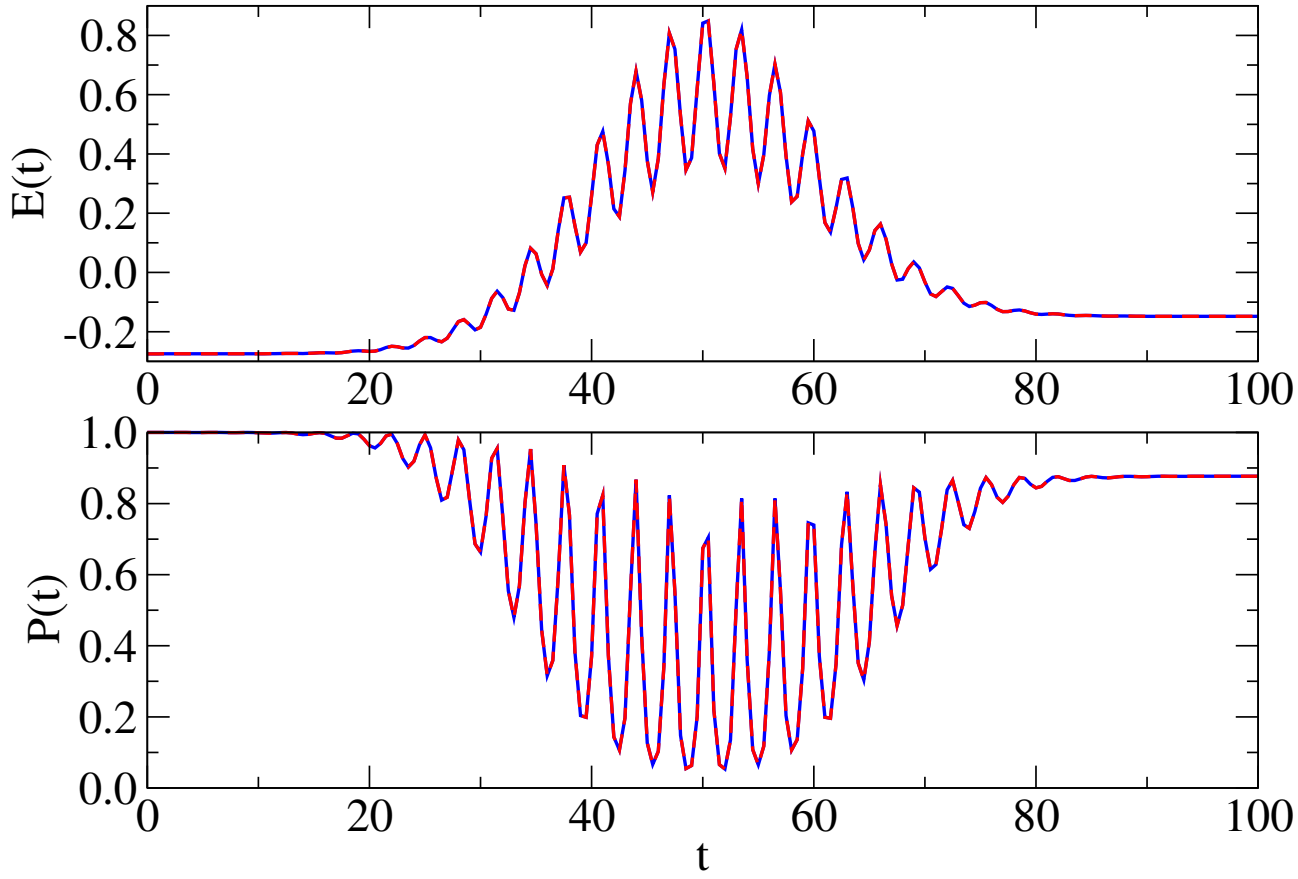

FIG. 9. Soft Coulomb potential with laser field B in 3D. Top: Energy as a function of time for grid (solid blue line), PWG (red dashed line). Bottom: Ground state occupation probability as a function of time for grid (solid blue line), PWG (red dashed line).

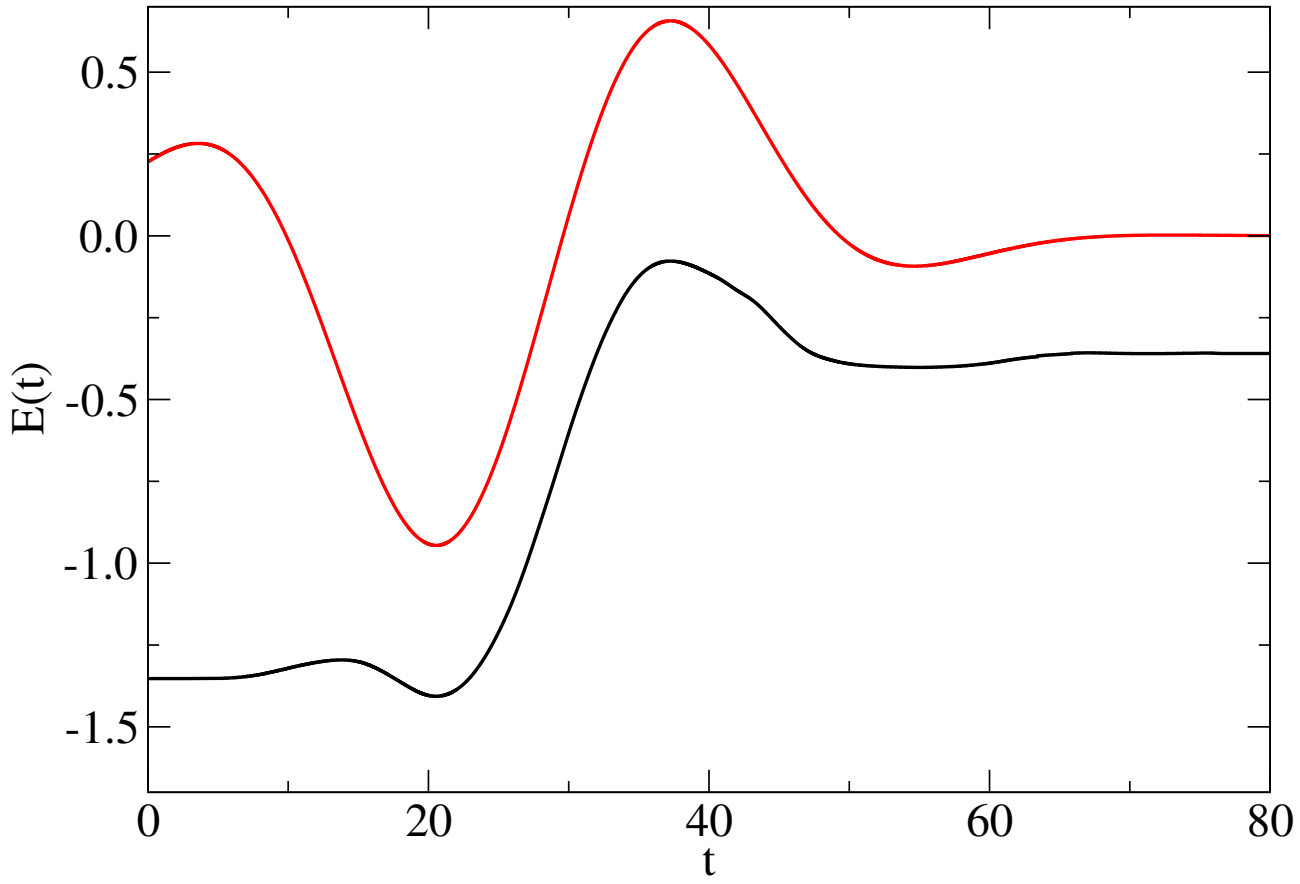

FIG. 10. Energy (black line) and laser field (dashed line) of a 2 electron system as a function of time. The laser parameters are $E_0 = 0.1, \tau = 20.5, \omega = 1.0, T = 25$. The amplitude of the laser on the figure is multiplied by 10 for better visibility.

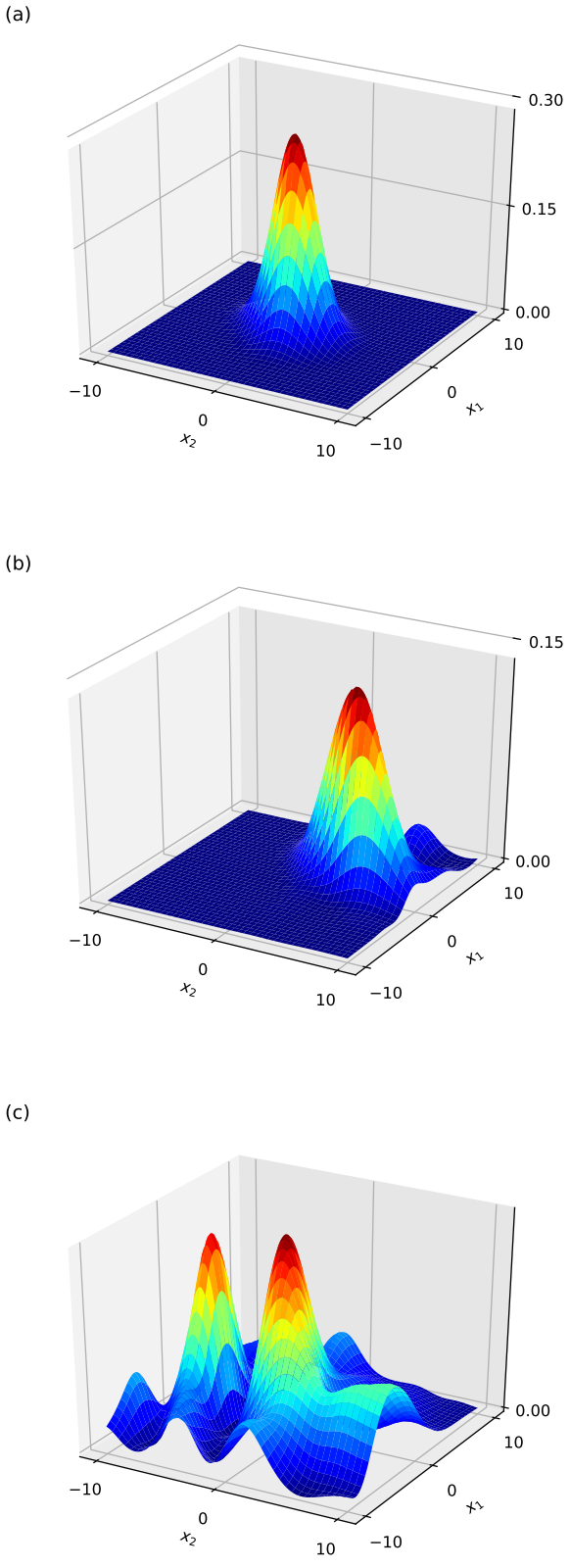

FIG. 11. Snapshots of the two electron density at (a) $t = 0$, (b) $t = 30$ and (c) $t = 50$ a.u.. The plane axis are x_1 and x_2, the coordinates of electron 1 and 2.

[1] F. Krausz and M. Ivanov, Rev. Mod. Phys. **81**, 163 (2009).
[2] K. Hütten, M. Mittermair, S. O. Stock, R. Beerwerth, V. Shirvanyan, J. Riemensberger, A. Duensing, R. Heider, M. S. Wagner, A. Guggenmos, S. Fritzsche, N. M. Kabachnik, R. Kienberger, and B. Bernhardt, Nature Communications **9**, 719 (2018).
[3] S. Cui, P.-L. He, and F. He, Phys. Rev. A **94**, 053401 (2016).
[4] M. A. Fareed, V. V. Strelkov, N. Thiré, S. Mondal, B. E. Schmidt, F. Légaré, and T. Ozaki, Nature Communications **8**, 16061 (2017).
[5] M. Kozák, J. McNeur, K. J. Leedle, H. Deng, N. Schönenberger, A. Ruehl, I. Hartl, J. S. Harris, R. L. Byer, and P. Hommelhoff, Nature Communications **8**, 14342 (2017).
[6] P. Peng, C. Marceau, and D. M. Villeneuve, Nature Reviews Physics **1**, 144 (2019).
[7] Y. Kobayashi, M. Reduzzi, K. F. Chang, H. Timmers, D. M. Neumark, and S. R. Leone, Phys. Rev. Lett. **120**, 233201 (2018).
[8] W. van Dijk and F. M. Toyama, Phys. Rev. E **90**, 063309 (2014).
[9] M. Nurhuda and F. H. M. Faisal, Phys. Rev. A **60**, 3125 (1999).
[10] A. Picón, Phys. Rev. A **95**, 023401 (2017).
[11] J. Bengtsson, E. Lindroth, and S. Selstø, Phys. Rev. A **78**, 032502 (2008).
[12] U. Peskin and N. Moiseyev, The Journal of Chemical Physics **99**, 4590 (1993).
[13] H. Gharibnejad, B. Schneider, M. Leadingham, and H. Schmale, Computer Physics Communications (2019), https://doi.org/10.1016/j.cpc.2019.05.019.
[14] B. Fetić and D. B. Milošević, Phys. Rev. E **95**, 053309 (2017).
[15] D. Wells and H. Quiney, Scientific Reports **9**, 782 (2019).
[16] K. Kormann, Communications in Computational Physics **20**, 6085 (2016).
[17] A. D. Bandrauk and H. Shen, The Journal of Chemical Physics **99**, 1185 (1993).
[18] E. Lötstedt, T. Kato, and K. Yamanouchi, Phys. Rev. A **99**, 013404 (2019).
[19] W. van Dijk, T. Vanderwoerd, and S.-J. Prins, Phys. Rev. E **95**, 023310 (2017).
[20] J. Kaushal and O. Smirnova, Phys. Rev. A **88**, 013421 (2013).
[21] P. V. Demekhin, D. Hochstuhl, and L. S. Cederbaum, Phys. Rev. A **88**, 023422 (2013).
[22] A. N. Grum-Grzhimailo, B. Abeln, K. Bartschat, D. Weflen, and T. Urness, Phys. Rev. A **81**, 043408 (2010).
[23] J. H. Bauer, F. Mota-Furtado, P. F. O'Mahony, B. Piraux, and K. Warda, Phys. Rev. A **90**, 063402 (2014).
[24] B. I. Schneider, Phys. Rev. A **55**, 3417 (1997).
[25] D. A. Horner, W. Vanroose, T. N. Rescigno, F. Martín, and C. W. McCurdy, Phys. Rev. Lett. **98**, 073001 (2007).
[26] L. Tao, C. W. McCurdy, and T. N. Rescigno, Phys. Rev. A **79**, 012719 (2009).
[27] H. Bachau, E. Cormier, P. Decleva, J. E. Hansen, and F. Martín, Reports on Progress in Physics **64**, 1815 (2001).
[28] W. Vanroose, D. A. Horner, F. Martín, T. N. Rescigno, and C. W. McCurdy, Phys. Rev. A **74**, 052702 (2006).
[29] J. Feist, S. Nagele, R. Pazourek, E. Persson, B. I. Schneider, L. A. Collins, and J. Burgdörfer, Phys. Rev. Lett. **103**, 063002 (2009).
[30] Y. Yu and B. D. Esry, Journal of Physics B: Atomic, Molecular and Optical Physics **51**, 095601 (2018).
[31] U. De Giovannini, A. H. Larsen, and A. Rubio, The European Physical Journal B **88**, 56 (2015).
[32] A. Scrinzi, Phys. Rev. A **81**, 053845 (2010).
[33] M. Weinmller, M. Weinmller, J. Rohland, and A. Scrinzi, Journal of Computational Physics **333**, 199 (2017).
[34] A. Scrinzi, H. Stimming, and N. Mauser, Journal of Computational Physics **269**, 98 (2014).
[35] P. A. M. Dirac, Mathematical Proceedings of the Cambridge Philosophical Society **26**, 376385 (1930).
[36] A. McLachlan, Molecular Physics **8**, 39 (1964).
[37] S. Sawada, R. Heather, B. Jackson, and H. Metiu, The Journal of Chemical Physics **83**, 3009 (1985).
[38] S. Rau, J. Main, H. Cartarius, P. Köberle, and G. Wunner, Phys. Rev. A **82**, 023611 (2010).
[39] J. O. Zoppe, M. L. Parkinson, and M. Messina, Chemical Physics Letters **407**, 308 (2005).
[40] T. c. v. Fabčič, J. Main, and G. Wunner, Phys. Rev. A **79**, 043417 (2009).
[41] G. Carleo, F. Becca, M. Schiró, and M. Fabrizio, Scientific Reports **2**, 243 EP (2012).
[42] K. Ido, T. Ohgoe, and M. Imada, Phys. Rev. B **92**, 245106 (2015).
[43] H. Feldmeier and J. Schnack, Rev. Mod. Phys. **72**, 655 (2000).
[44] E. Deumens, A. Diz, R. Longo, and Y. Öhrn, Rev. Mod. Phys. **66**, 917 (1994).
[45] R. Anzaki, T. Sato, and K. L. Ishikawa, Phys. Chem. Chem. Phys. **19**, 22008 (2017).
[46] J. Mitroy, S. Bubin, W. Horiuchi, Y. Suzuki, L. Adamowicz, W. Cencek, K. Szalewicz, J. Komasa, D. Blume, and K. Varga, Rev. Mod. Phys. **85**, 693 (2013).
[47] Y. Suzuki and K. Varga, *Stochastic variational Approach to Quantum-Mechanical Few-Body Problems*, 172 (Springer, New York, 1998).
[48] K. Varga, Phys. Rev. A **99**, 012504 (2019).
[49] C. Marante, L. Argenti, and F. Martín, Phys. Rev. A **90**, 012506 (2014).
[50] M. Cafiero, S. Bubin, and L. Adamowicz, Phys. Chem. Chem. Phys. **5**, 14911501 (2003).
[51] S. Bubin, M. Pavanello, W.-C. Tung, K. L. Sharkey, and L. Adamowicz, Chemical Reviews **113**, 3679 (2013), pMID: 23020161, http://dx.doi.org/10.1021/cr200419d.
[52] A. K. Kazansky, Journal of Physics B: Atomic, Molecular and Optical Physics **31**, L579 (1998).
[53] C. Leforestier, R. Bisseling, C. Cerjan, M. Feit, R. Friesner, A. Guldberg, A. Hammerich, G. Jolicard, W. Karrlein, H.-D. Meyer, N. Lipkin, O. Roncero, and R. Kosloff, J. Comput. Phys. **94**, 59 (1991).
[54] H. Tal-Ezer and R. Kosloff, J. Chem. Phys. **81**, 3967 (1984).
[55] D. Kosloff and R. Kosloff, J. Comput. Phys. **52**, 35 (1983).
[56] A. Gordon, C. Jirauschek, and F. X. Kärtner, Phys. Rev. A **73**, 042505 (2006).
[57] G. Palma and U. Raff, Canadian Journal of Physics **84**, 787 (2006).
[58] X. Zhou and C. D. Lin, Phys. Rev. A **61**, 053411 (2000).
[59] V. C. Reed and K. Burnett, Phys. Rev. A **42**, 3152 (1990).

[60] K. Varga and J. A. Driscoll, *Computational Nanoscience* (Cambridge University Press, New York, 2011).
[61] A. Pohl, P.-G. Reinhard, and E. Suraud, Phys. Rev. Lett. **84**, 5090 (2000).
[62] U. De Giovannini, D. Varsano, M. A. L. Marques, H. Appel, E. K. U. Gross, and A. Rubio, Phys. Rev. A **85**, 062515 (2012).

Appendix A: Propagation of a free Gaussian wave packet

To illustrate the time propagation on a simple example, we consider the time evolution of a Gaussian wave packet in 1D. The Hamiltonian is:

$$H = -\frac{1}{2}\frac{\partial^2}{\partial x^2}, \tag{A1}$$

and the trial function is written in the form Defining a one dimensional Gaussian as:

$$g = e^{\gamma - \alpha x^2 - \kappa x}, \tag{A2}$$

. The derivatives with respect to the parameters are:

$$\frac{\partial g}{\partial \gamma} = g, \quad \frac{\partial g}{\partial \alpha} = -x^2 g, \quad \frac{\partial g}{\partial \kappa} = -xg, \tag{A3}$$

so the M matrix (see Eq. (10)) is:

$$M = \begin{pmatrix} \langle g|g\rangle & -\langle g|x^2|g\rangle & -\langle g|x|g\rangle \\ -\langle g|x^2|g\rangle & \langle g|x^4|g\rangle & \langle g|x^3|g\rangle \\ -\langle g|x|g\rangle & \langle g|x^3|g\rangle & \langle g|x^2|g\rangle \end{pmatrix}. \tag{A4}$$

The action of the Hamiltonian on the trial function can be expressed as:

$$Hg = -\frac{1}{2}\frac{\partial^2 g}{\partial x^2} = \left((\alpha - \kappa^2/2) - 2\alpha^2 x^2 - 2\alpha\kappa x\right) g. \tag{A5}$$

The **v** vector is defined as:

$$\mathbf{v} = \begin{pmatrix} \langle g|H|g\rangle \\ -\langle g|x^2 H|g\rangle \\ -\langle g|xH|g\rangle \end{pmatrix}, \tag{A6}$$

which can be rewritten using Eq. (A5) and the definition of M as:

$$\mathbf{v} = M \begin{pmatrix} \alpha - \kappa^2/2 \\ 2\alpha^2 \\ 2\alpha\kappa \end{pmatrix}. \tag{A7}$$

Using this Eq. (12) becomes:

$$iM \begin{pmatrix} \dot\gamma \\ \dot\alpha \\ \dot\kappa \end{pmatrix} = M \begin{pmatrix} \alpha - \kappa^2/2 \\ 2\alpha^2 \\ 2\alpha\kappa \end{pmatrix}. \tag{A8}$$

The equation for α,

$$i\dot\alpha = 2\alpha^2, \tag{A9}$$

can be integrated easily:

$$\alpha(t) = \frac{\alpha(0)}{2i\alpha(0)t + 1}. \tag{A10}$$

Substituting this into

$$i\dot\kappa = 2\alpha\kappa, \tag{A11}$$

we get

$$\kappa(t) = \frac{\kappa(0)}{2i\alpha(0)t + 1}. \tag{A12}$$

Now using

$$i\dot\gamma = \alpha - \kappa^2/2, \tag{A13}$$

we get

$$\gamma(t) = -\frac{1}{2}\ln(2i\alpha(0)t + 1) + \frac{i\kappa(0)^2 t}{4i\alpha(0)t + 2} + \gamma(0). \tag{A14}$$

The solution agrees with the analytical solution of time propagation of Gaussian wave packets.

Appendix B: Matrix elements: 1D PTG

For simplicity, first we calculate the matrix elements for a single basis function:

$$g = z^n e^{\gamma - \beta z^2}, \tag{B1}$$

and the we show how to generalize the results for N basis functions. Instead of using using the linear coefficient c we use $c = e^\gamma$, which makes the equations simpler: The derivative of the exponential function is proportional to the exponential so the basis function remains in the same

form. In the ground state calculations, c is a real number, so to initialize γ we set $\mathrm{Im}(\gamma) = 0$ if $c > 0$ and $\mathrm{Im}(\gamma = \pi)$ if $c < 0$. Alternatively, one can write the matrix elements in terms of γ and switch back to c in the numerical work.

We take the derivatives with respect to the parameters:

$$\frac{dg}{d\gamma} = g \tag{B2}$$

$$\frac{dg}{d\beta} = -z^2 g. \tag{B3}$$

We then get the matrix M from Eq. (10):

$$M = \begin{pmatrix} \langle g|g\rangle & -\langle g|z^2|g\rangle \\ -\langle g|z^2|g\rangle & \langle g|z^4|g\rangle \end{pmatrix}. \tag{B4}$$

Then $\mathbf{v}$ is defined as:

$$\mathbf{v} = \begin{pmatrix} \langle g|H|g\rangle \\ -\langle g|z^2 H|g\rangle \end{pmatrix}. \tag{B5}$$

To calculate these matrix elements we need the action of the kinetic energy operator on g:

$$-\frac{1}{2}\frac{\partial^2 g}{\partial z^2} = \left(-\frac{1}{2}n(n-1)z^{-2} + (2n+1)\beta - 2\beta^2 z^2\right) g. \tag{B6}$$

The generalization for N basis functions, $g_1, \ldots, g_N$ is simple. The M matrix in Eq. (B4) will now be built up in $N \times N$ block matrices:

$$M = \begin{pmatrix} \langle g_i|g_j\rangle & -\langle g_i|\, z^2\, |g_j\rangle \\ -\langle g_i|\, z^2\, |g_j\rangle & \langle g_i|\, z^4\, |g_j\rangle \end{pmatrix}. \tag{B7}$$

Similarly for $\mathbf{v}$ we have:

$$\mathbf{v} = \begin{pmatrix} \sum_{k=1}^{N} \langle g_i|\, H\, |g_k\rangle \\ -\sum_{k=1}^{N} \langle g_i|\, z^2 H\, |g_k\rangle \end{pmatrix}. \tag{B8}$$

Now we assume a general potential can be expanded in terms of Gaussians:

$$V(z) = \sum_i v_i e^{-v_z^i z^2}. \tag{B9}$$

In this case all the necessary matrix elements can be derived from:

$$\langle g_\sigma|z^k e^{-\nu z^2}|g_{\sigma'}\rangle = e^{\gamma^* + \gamma'} \frac{(k-1)!!\sqrt{\pi}}{(\sigma^* + \sigma' + \nu)^{(k+1)/2} 2^{(k/2)}} \tag{B10}$$

if k is even and zero otherwise. Note this formula is valid if the integral is convergent, which in turn is true if $\mathrm{Re}(\sigma^* + \sigma' + \nu) > 0$. The principal value square root should be used in Eq. (B10).

Appendix C: Matrix elements: 3D PTG

In this section we calculate the matrix elements for a PTG basis function:

$$g = z^n e^{\gamma - \alpha(x^2+y^2) - \beta z^2}. \tag{C1}$$

We need the derivatives with respect to the parameters:

$$\frac{\partial g}{\partial \gamma} = g, \tag{C2}$$

$$\frac{\partial g}{\partial \alpha} = -(x^2+y^2) g, \tag{C3}$$

$$\frac{\partial g}{\partial \beta} = -z^2 g. \tag{C4}$$

To calculate these matrix elements we need the action of the kinetic energy operator on g:

$$-\frac{1}{2}\left(\frac{\partial^2}{\partial x^2} + \frac{\partial^2}{\partial y^2}\right) g = \left(2\alpha - 2\alpha^2(x^2+y^2)\right) g, \tag{C5}$$

$$-\frac{1}{2}\frac{\partial^2 g}{\partial z^2} = \left(-\frac{1}{2}n(n-1)z^{-2} + (2n+1)\beta - 2\beta^2 z^2\right) g. \tag{C6}$$

The M matrix in Eq. (10) will now be built up $N \times N$ block matrices:

$$M = \begin{pmatrix} \langle g_i|g_j\rangle & -\langle g_i|x^2+y^2|g_j\rangle & -\langle g_i|z^2|g_j\rangle \\ -\langle g_i|x^2+y^2|g_j\rangle & \langle g_i|(x^2+y^2)^2|g_j\rangle & \langle g_i|(x^2+y^2)z^2|g_j\rangle \\ -\langle g_i|z^2|g_j\rangle & \langle g_i|(x^2+y^2)z^2|g_j\rangle & \langle g_i|z^4|g_j\rangle \end{pmatrix}. \tag{C7}$$

Similarly, for the $\mathbf{v}$ vector we have:

$$\mathbf{v} = \begin{pmatrix} \sum_{k=1}^{N} \langle g_i|H|g_k\rangle \\ -\sum_{k=1}^{N} \langle g_i|(x^2+y^2)H|g_k\rangle \\ -\sum_{k=1}^{N} \langle g_i|z^2 H|g_k\rangle \end{pmatrix}, \tag{C8}$$

where each entry corresponds to a $N \times 1$ block matrix.

Now we will assume, that a general potential can be expanded in terms of Gaussians:

$$V(x,y,z) = \sum_i v_i e^{-\nu_x^i x^2 - \nu_y^i y^2 - \nu_z^i z^2}. \tag{C9}$$

For spherically symmetric potentials this expansion further simplifies:

$$V(r) = \sum_i v_i e^{-\nu^i (x^2+y^2+z^2)}. \tag{C10}$$

In case of Gaussian potentials, all the necessary matrix elements of M and $\mathbf{v}$ can be derived from:

$$\langle g_{\sigma_x}|x^{k_x}e^{-\nu_x x^2}|g_{\sigma'_x}\rangle\langle g_{\sigma_y}|y^{k_y}e^{-\nu_y y^2}|g_{\sigma'_y}\rangle\langle g_{\sigma_z}|z^{k_z}e^{-\nu_z z^2}|g_{\sigma'_z}\rangle \tag{C11}$$

The one dimensional integral can be easily calculated as above in Eq. (B10).

One can also calculate the matrix elements analytically for the 3D Coulomb potential:

$$V(r) = -\frac{1}{\sqrt{x^2+y^2+z^2}} \tag{C12}$$

We can calculate the necessary matrix elements using the following integral identity:

$$\frac{1}{\sqrt{x^2+y^2+z^2}} = \frac{2}{\sqrt{\pi}}\int_0^\infty e^{-u^2(x^2+y^2+z^2)}du. \tag{C13}$$

This allows us to evaluate the integral:

$$\langle g|\,V(x,y,z)\,|g'\rangle = -\frac{2}{\sqrt{\pi}}e^{\gamma^*+\gamma'}\int_0^\infty du\int_{-\infty}^\infty\int_{-\infty}^\infty\int_{-\infty}^\infty z^{n+n'}e^{-(u^2+a)(x^2+y^2)-(u^2+b)z^2}dxdydz, \tag{C14}$$

where

$$a = \alpha^* + \alpha', b = \beta^* + \beta'. \tag{C15}$$

With $n+n'=0$ (C14) yields:

$$\langle g|\,V(x,y,z)\,|g'\rangle = -2\pi e^{\gamma^*+\gamma'}\frac{\arccos\left(\frac{\sqrt{a}}{\sqrt{b}}\right)}{\sqrt{a}\sqrt{b}\sqrt{1-\frac{a}{b}}}, \tag{C16}$$

where $\mathrm{Re}(a)>0$ and $\mathrm{Re}(b)>0$. In the case that $a=b$:

$$\langle g|\,V(x,y,z)\,|g'\rangle = -\frac{2\pi}{a}e^{\gamma^*+\gamma'}. \tag{C17}$$

Note that (C14) will be 0 when the polynomial terms are of odd degree. We can thus evaluate the more general form by taking derivatives as follows:

$$(-1)^n\frac{\partial^n}{\partial a^n}\langle g|\,V(x,y,z)\,|g'\rangle = \langle g|\,(x^2{+}y^2)^n V(x,y,z)\,|g'\rangle\,, \tag{C18}$$

$$(-1)^n\frac{\partial^n}{\partial b^n}\langle g|\,V(x,y,z)\,|g'\rangle = \langle g|\,z^{2n} V(x,y,z)\,|g'\rangle\,, \tag{C19}$$

$$\frac{\partial^{2n}}{(\partial a\partial b)^n}\langle g|\,V(x,y,z)\,|g'\rangle = \langle g|\,(x^2{+}y^2)^n z^{2n} V(x,y,z)\,|g'\rangle\,. \tag{C20}$$

When $a=b$, the form (C16) cannot be evaluated. In this case, (C14) simplifies considerably into a form which can be easily evaluated and yields simple polynomial answers [47].

Appendix D: Matrix elements: 3D PWG

In this case we have the basis function in the form:

$$g = e^{\gamma-\alpha(x^2+y^2)-\beta z^2+kz}. \tag{D1}$$

The M matrix in Eq. (10) will now be built up $N\times N$ block matrices:

$$M = \begin{pmatrix} \langle g_i|g_j\rangle & -\langle g_i|x^2+y^2|g_j\rangle & -\langle g_i|z^2|g_j\rangle & \langle g_i|z|g_j\rangle \\ -\langle g_i|x^2+y^2|g_j\rangle & \langle g_i|(x^2+y^2)^2|g_j\rangle & \langle g_i|(x^2+y^2)z^2|g_j\rangle & -\langle g_i|(x^2+y^2)z|g_j\rangle \\ -\langle g_i|z^2|g_j\rangle & \langle g_i|(x^2+y^2)z^2|g_j\rangle & \langle g_i|z^4|g_j\rangle & -\langle g_i|z^3|g_j\rangle \\ \langle g_i|z|g_j\rangle & -\langle g_i|(x^2+y^2)z|g_j\rangle & -\langle g_i|z^3|g_j\rangle & \langle g_i|z^2|g_j\rangle \end{pmatrix}. \tag{D2}$$

Similarly, for the $\mathbf{v}$ vector we have:

$$\mathbf{v} = \begin{pmatrix} \sum_{k=1}^{N} \langle g_i|H|g_k\rangle \\ -\sum_{k=1}^{N} \langle g_i|(x^2+y^2)H|g_k\rangle \\ -\sum_{k=1}^{N} \langle g_i|z^2H|g_k\rangle \\ \sum_{k=1}^{N} \langle g_i|zH|g_k\rangle \end{pmatrix}. \tag{D3}$$

All the necessary matrix elements can then be calculated from Eq. (C11) using Eq. (B10) provided that the potential is expanded into Gaussians. The matrix elements for 1D PWG can be obtained by taking $\alpha = 0$ and eliminating the second row and column from M, and the second row from $\mathbf{v}$.